Elastic Scattering of Alpha Particles by N^{15}†

H. SMOTRICH, K. W. JONES,* L. C. McDERMOTT, AND R. E. BENENSON‡

Columbia University, New York, New York

(Received August 24, 1960)

Absolute differential cross sections for the elastic scattering of alpha particles by N^{15} have been measured in a differentially-pumped gas scattering chamber. The measurements were made at center-of-mass angles of 169.1, 149.5, 140.8, 125.3, 90.0, and 70.0 degrees for alpha-particle energies from 1.75 to 5.50 Mev, corresponding to 5.37- to 8.33-Mev excitation of the compound nucleus F^{19}. The experimental widths of the levels observed below approximately 3.5-Mev bombarding energy are generally narrow, in most cases less than 10 kev. Above 3.5 Mev a marked increase in the level width was observed. As a result of an analysis based on the Wigner-Eisenbud reaction theory, values of J, π, E_λ, and γ_λ^2 were assigned to 16 levels in F^{19}.

I. INTRODUCTION

RECENTLY, the energies, spins, and parities of the low-lying levels of F^{19} have been derived from calculations based on the shell model[1-4] and the rotational model.[5,6] Full confirmation of these calculations has been limited to the levels below approximately 1.5 Mev for which experimental spin and parity information is available. The success of these theoretical calculations, coupled with the general lack of spin and parity data, has stimulated interest in experiments which would contribute further information on the higher states. At the time of the present experiment, level positions were quite well known up to 5-Mev excitation, and spin and parity assignments had been made to the levels below approximately 1.5 Mev.[7-12] The region from 5 to 8 Mev had been explored and the positions of a few levels were known, but there was virtually no information on the spins and parities of the levels. A study of the elastic scattering of alpha particles by N^{15} was made in the present experiment in order to locate and determine the properties of $T=\frac{1}{2}$ levels of F^{19} in this energy region. For bombarding energies up to 5.031 Mev, elastic scattering and capture are the only energetically possible processes. Furthermore, since the spin of N^{15} is $\frac{1}{2}$ and the spin of the alpha particle is zero, the results can be readily analyzed in terms of Wigner-Eisenbud reaction theory

to obtain the level spins, parities, and reduced widths. Such assignments may also be useful in the study of lower lying levels of F^{19} through the capture reaction $N^{15}(\alpha,\gamma)F^{19}$.

II. APPARATUS

The small-volume scattering chamber used in measuring the absolute differential cross sections for the elastic scattering of alpha particles by N^{15} is shown in Fig. 1. The scattering chamber was separated from the Van de Graaff accelerator by a three-stage differential pumping column (only the first stage is shown in Fig. 1). This differential pumping column served as a thin entrance window to the scattering volume and as a collimator for the singly charged alpha-particle beam from the Van de Graaff accelerator. The angular spread of the beam defined by the entrance and exit apertures of the pumping column was ± 0.15 degree. The scattering chamber and associated gas handling equipment required approximately 100 atom-cc of gas to obtain target pressures of the order of 0.3 cm Hg.

An analyzing magnet calibrated with the $Li^7(p,n)Be^7$ reaction was used to determine the energy of the incident beam to approximately $\pm 0.1\% E$. The energy resolution, as estimated from the magnet entrace and exit slit dimensions,[13] and from the widths of narrow resonances, was also about 0.1% of the beam energy.

The alpha-particle beam, after traversing the differential pumping column and the scattering volume, passed through a thin (25×10^{-6} inch) nickel window into an evacuated collector cup. The collector cup had electric and magnetic fields applied to it in order to suppress secondary electrons. A sensitive current integrator[14] was used to determine the amount of charge collected. The line source of scattered alpha particles was defined by a set of rectangular slits with a half-angle aperture of approximately 2 degrees. The scattered alpha particles were detected by a thin (2-3 mils thick) CsI(Tl) crystal mounted on a Dumont 6291 photomultiplier tube. The detector and defining slits were mounted as a unit in the rotating head of the scattering

† This work partially supported by the U. S. Atomic Energy Commission.

* Now at The Ohio State University, Columbus, Ohio.

‡ Permanent address: City College of New York, New York, New York.

[1] J. P. Elliott and B. H. Flowers, Proc. Roy. Soc. (London) A229, 536 (1955).

[2] M. G. Redlich, Phys. Rev. 95, 448 (1954).

[3] M. G. Redlich, Phys. Rev. 99, 1427 (1955).

[4] M. G. Redlich, Phys. Rev. 110, 468 (1958).

[5] E. B. Paul, Phil. Mag. 15, 311 (1957).

[6] G. Rakavy, Nuclear Phys. 4, 375 (1957).

[7] F. Ajzenberg-Selove and T. Lauritsen, Nuclear Phys. 11, 1 (1959).

[8] B. J. Toppel, D. H. Wilkinson, and D. E. Alburger, Phys. Rev. 101, 1485 (1956).

[9] P. C. Price, Proc. Phys. Soc. (London) A70, 661 (1957).

[10] M. V. Harlow, J. B. Marion, and R. A. Chapman, Phys. Rev. 101, 214 (1956).

[11] J. W. Butler and H. D. Holmgren, Phys. Rev. 112, 461 (1958); J. W. Butler, L. W. Fagg, and H. D. Holmgren, Phys. Rev. 113, 268 (1959).

[12] A. Hossain and A. N. Kamal, Phys. Rev. 108, 390 (1957).

[13] H. Smotrich, Ph.D. dissertation, Columbia University, 1959 (unpublished); R. F. Taschek, Rev. Sci. Instr. 19, 591 (1948).

[14] G. M. B. Bouricius and F. C. Shoemaker, Rev. Sci. Instr. 22, 183 (1951).
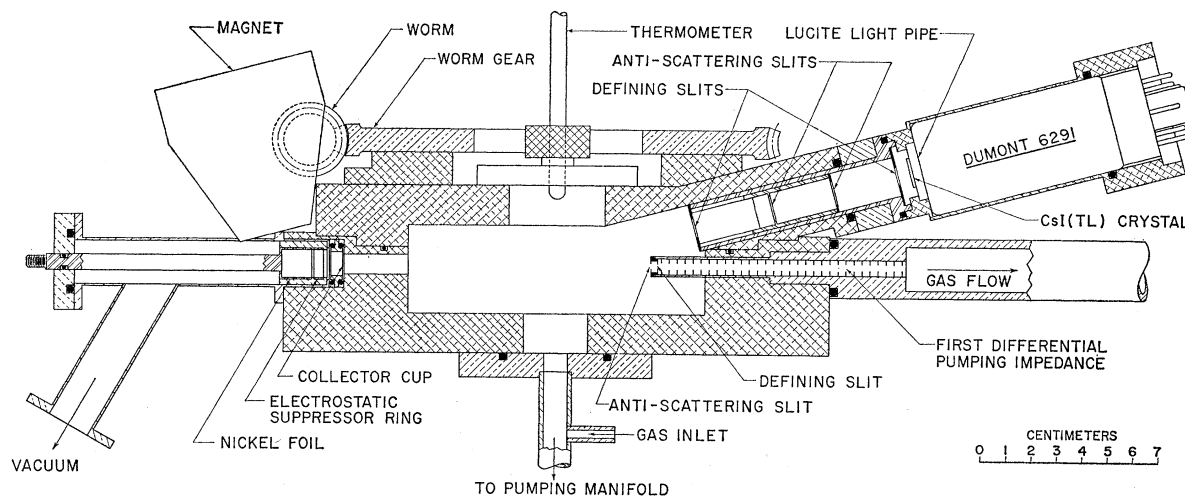
FIG. 1. Cross-section view of the small-volume gas scattering chamber.

chamber at an angle of 14.8 degrees with the horizontal. It was possible to rotate the scattering chamber head continuously through 360 degrees, permitting measurements to be made at laboratory scattering angles from 14.8 to 165.2 degrees. These angles were set to the nearest 0.1 degree by means of an angle vernier. The accuracy of the scattering angle setting was estimated from a measurement of the $O^{16}(p,p)O^{16}$ cross section at $\theta_{lab}=40°$ and $E_p=0.95$ Mev. At this angle and energy, the angular dependence of the cross section is well

represented by $csc^4(\theta/2)$. The maximum uncertainty in scattering angle was estimated to be $\pm0.2°$ from this data. By allowing for rotation of the counter assembly about the detector axis, it was possible to orient the long dimension of the rectangular counter slits perpendicular to the scattering plane defined by the beam direction and the counter axis. This procedure resulted in a uniform scattering geometry at all scattering angles and accordingly a great simplification in the analysis of the scattering data.
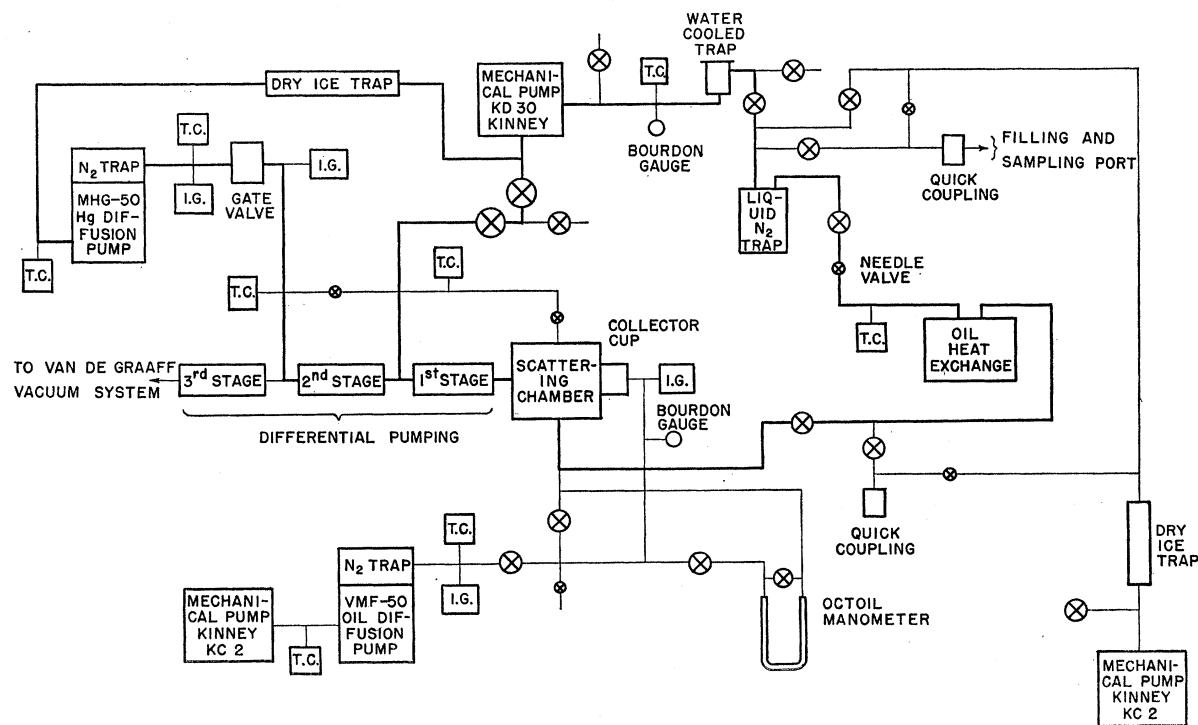

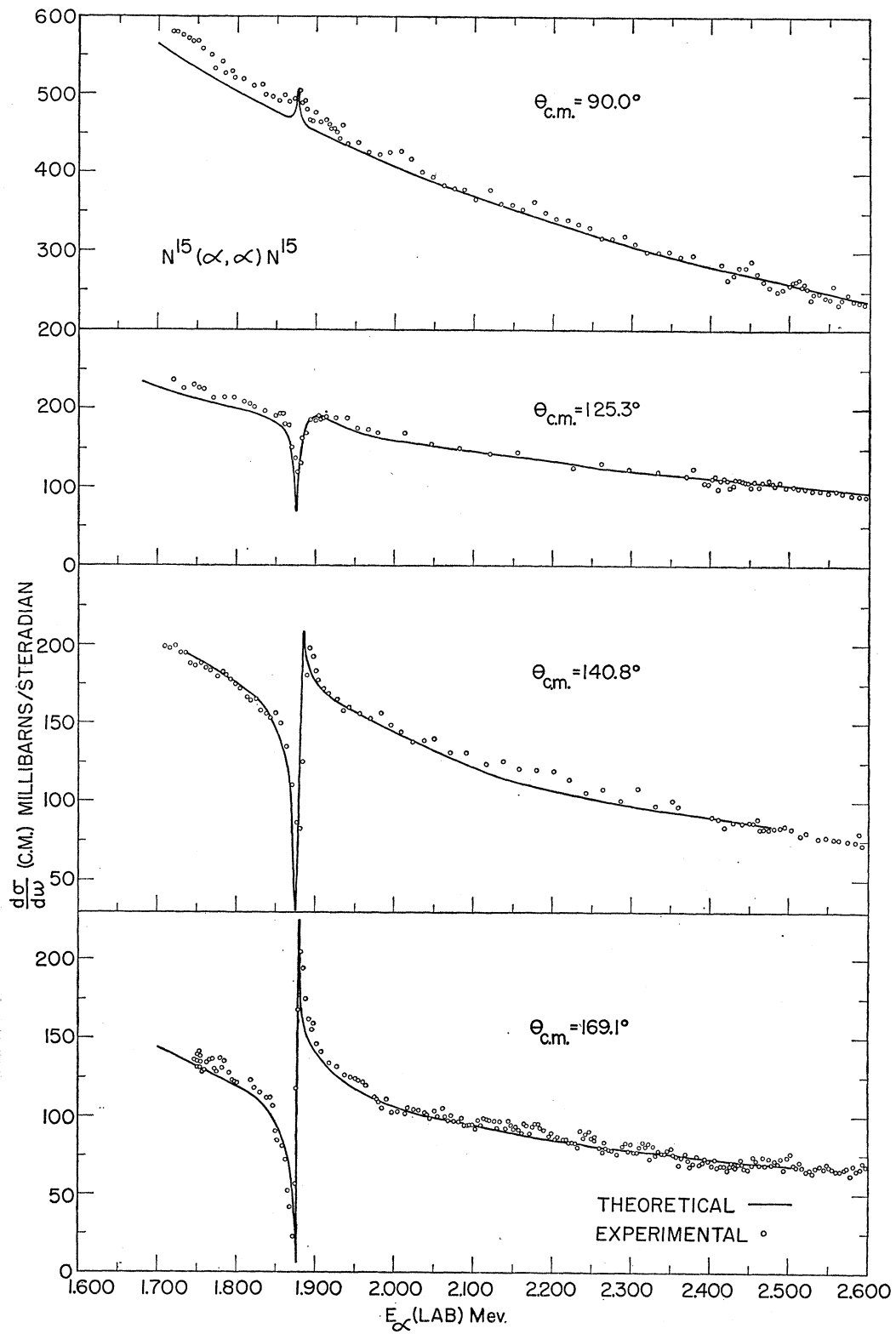FIG. 2. Schematic diagram of gas recirculating system.

FIG. 3. Experimental and theoretical differential cross sections from 1.7 Mev to 2.6 Mev.

In order to reduce the amount of N¹⁵ gas lost from the system, the gas pumped out of the first two stages of the differential pumping column was recirculated. The target gas recirculation system and vacuum system used in the experiment are shown in Fig. 2.

The N¹⁵ target gas was produced by a chemical exchange process developed by Spindel and Taylor.[15] This process can give isotopic concentrations of N¹⁵ in excess of 99 atom percent. The isotopic abundance of N¹⁵ was monitored throughout the course of the experiment by mass-spectrometric analyses, and indicated an average N¹⁵ concentration of 95 atom percent. The major contaminants were O¹⁶ and N¹⁴. Periodic checks for C¹² and H₂ contamination indicated the presence of these elements in trace quantities. The possibility that some of the levels observed in the present experiment were due to scattering from N¹⁴ or O¹⁶ can be eliminated (with exception for N¹⁴ in the uninvestigated region from $E_\alpha = 4.7$ Mev to $E_\alpha = 5.5$ Mev) by comparison with the results of N¹⁴(α,α)N¹⁴ experiments[16,17] and O¹⁶(α,α)O¹⁶ experiments.[18,19] In most cases the energies of the resonances found in N¹⁵(α,α)N¹⁵ did not agree with those found for alpha-particle scattering from N¹⁴ and O¹⁶. In cases where there was close agreement in energy, comparison of cross sections, shapes, and level widths established that the resonance was due to N¹⁵. Contamination of the target gas caused a maximum uncertainty of ±5% in the absolute cross section.

The error in current integration introduced by small-angle Coulomb scattering[20] of the alpha-particle beam by the target gas and collector cup entrance foil has been estimated and found to be less than 0.5%.

III. EXPERIMENTAL PROCEDURE AND RESULTS

Excitation curves were run at six angles in energy steps from 2 to 5 kev and covered the energy range from 1.75 to 5.50 Mev. The target thicknesses were varied in the range from 2 to 4 kev depending on the cross section. The selection of the scattering angles was governed by the dependence of the coherent scattering amplitude [see Eq. (1b)] on the orbital angular momentum l. This procedure was followed since it is possible to obtain an indication of the l value responsible for a particular resonance by the disappearance of an anomaly in the excitation curve at the scattering angle corresponding to a zero of the Legendre polynomial. In the present experiment the center-of-mass angles and the corresponding Legendre polynomial zeroes are: 149.5° and 70.0°, $P_4 = 0$; 140.8°, $P_3 = 0$; 125.3°, $P_2 = 0$; and 90.0°, all odd

[15] W. Spindel and T. I. Taylor, J. Chem. Phys. 24, 626 (1956).
[16] D. F. Herring, Ren Chiba, B. R. Gasten, and H. T. Richards, Phys. Rev. 112, 1210 (1958).
[17] E. Kashy, P. D. Miller, and J. R. Risser, Phys. Rev. 112, 547 (1958).
[18] J. R. Cameron, Phys. Rev. 90, 839 (1953).
[19] L. C. McDermott, K. W. Jones, H. Smotrich, and R. E. Benenson, Phys. Rev. 118, 175 (1960).
[20] W. C. Dickenson and D. C. Dodder, Rev. Sci. Instr. 24, 428 (1953).

Legendre polynomials vanish. Measurements were also taken at 169.1° where all Legendre polynomials are nonvanishing.

The computation of the absolute cross sections and bombarding energies from the experimental data was performed with an IBM 650 digital computer. The final cross-section curves are shown in Figs. 3–6. The curves drawn through the data points are the curves calculated from the application of Wigner-Eisenbud reaction theory.

The average over-all rms error on the measured cross sections is estimated at about 6.2%. A summary of the various sources of error is given in Table I.

Uncertainties in the alpha-particle energy scale arise from ±0.1% uncertainty in the energy calibration constant for the analyzing magnet and from the difficulty of accurately measuring the amount of energy lost in the differential pumping column. For typical experimental conditions, the uncertainty in the energy scale is slightly greater than ±0.1%.

IV. ANALYSIS

A. Technique

In the analysis of the differential cross sections it has been assumed that the capture cross section is negligible compared to the elastic scattering cross section. The differential cross section for the scattering of spin-zero particles by spin-$\frac{1}{2}$ nuclei is given by the expression[21]

$$d\sigma/d\omega = (1/k^2)[|A|^2 + |B|^2], \quad (1a)$$

where

$$A = -\tfrac{1}{2}\eta \csc^2(\theta/2) \exp[i\eta \ln \csc^2(\theta/2)]$$

$$+ \sum_{l=0}^{\infty} [(l+1) \sin\delta_l^+ \exp(i\delta_l^+)$$

$$+ l \sin\delta_l^- \exp(i\delta_l^-)]P_l(\cos\theta) \exp(i\alpha_l), \quad (1b)$$

$$B = \sin\theta[\sum_{l=1}^{\infty} [\sin\delta_l^+ \exp(i\delta_l^+)$$

$$- \sin\delta_l^- \exp(i\delta_l^-)]P_l'(\cos\theta) \exp(i\alpha_l)]. \quad (1c)$$

In these expressions θ is the scattering angle in the

TABLE I. Summary of errors for absolute cross-section measurements.

Geometry	±0.28%
Average counting statistics	±3.0%
Average uncertainty in background	±1.0%
Maximum angular uncertainty	±1.3%
Current integration	±0.7%
Average gas pressure uncertainty	±0.5%
Maximum uncertainty in absolute cross section from target gas impurities	±5.0%
Rms error	±6.2%

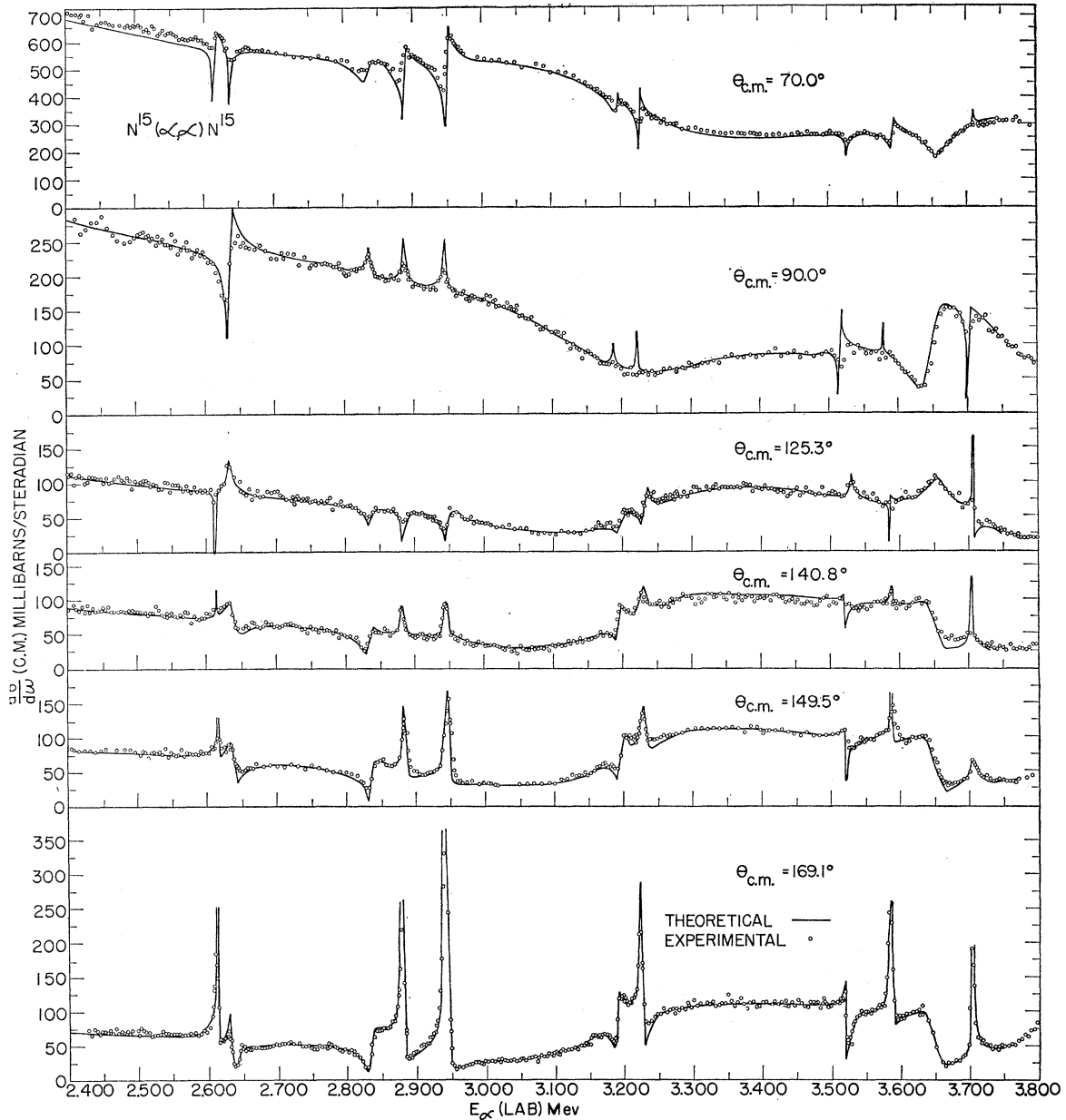[21] C. L. Critchfield and D. C. Dodder, Phys. Rev. 76, 602 (1949).

FIG. 4. Experimental and theoretical differential cross sections from 2.4 Mev to 3.8 Mev.

center-of-mass system, $\delta_l^{\pm}$ is the non-Coulomb phase shift of the partial wave of orbital angular momentum $l\hbar$ and total angular momentum $j=(l\pm\frac{1}{2})\hbar$. The quantities $k=1/\lambda$ and η are related to the reduced mass μ and the relative velocity v of the scattering pair by the expressions

$$k=1/\lambda=\mu v/\hbar, \qquad (2a)$$

$$\eta=ZZ'e^2/\hbar v. \qquad (2b)$$

The quantity α_l, which is the phase shift due to pure

Coulomb scattering, is given by the expression

$$\exp(i\alpha_l)=\prod_{s=1}^{l}\left(\frac{s+i\eta}{s-i\eta}\right)=\exp\left[2i\sum_{s=1}^{l}\tan^{-1}(\eta/s)\right], \quad (3)$$

for $l>1$. For $l=0$, $\exp(i\alpha_0)=1$. Finally $P_l(\cos\theta)$ is the Legendre polynomial of order l and $P_l'(\cos\theta)$ is the derivative of the Legendre polynomial with respect to $\cos\theta$.

The term A in Eq. (1a) arises from the coherent addition of the Coulomb and nuclear scattering amplitudes; term B in Eq. (1a) arises from scattering processes in
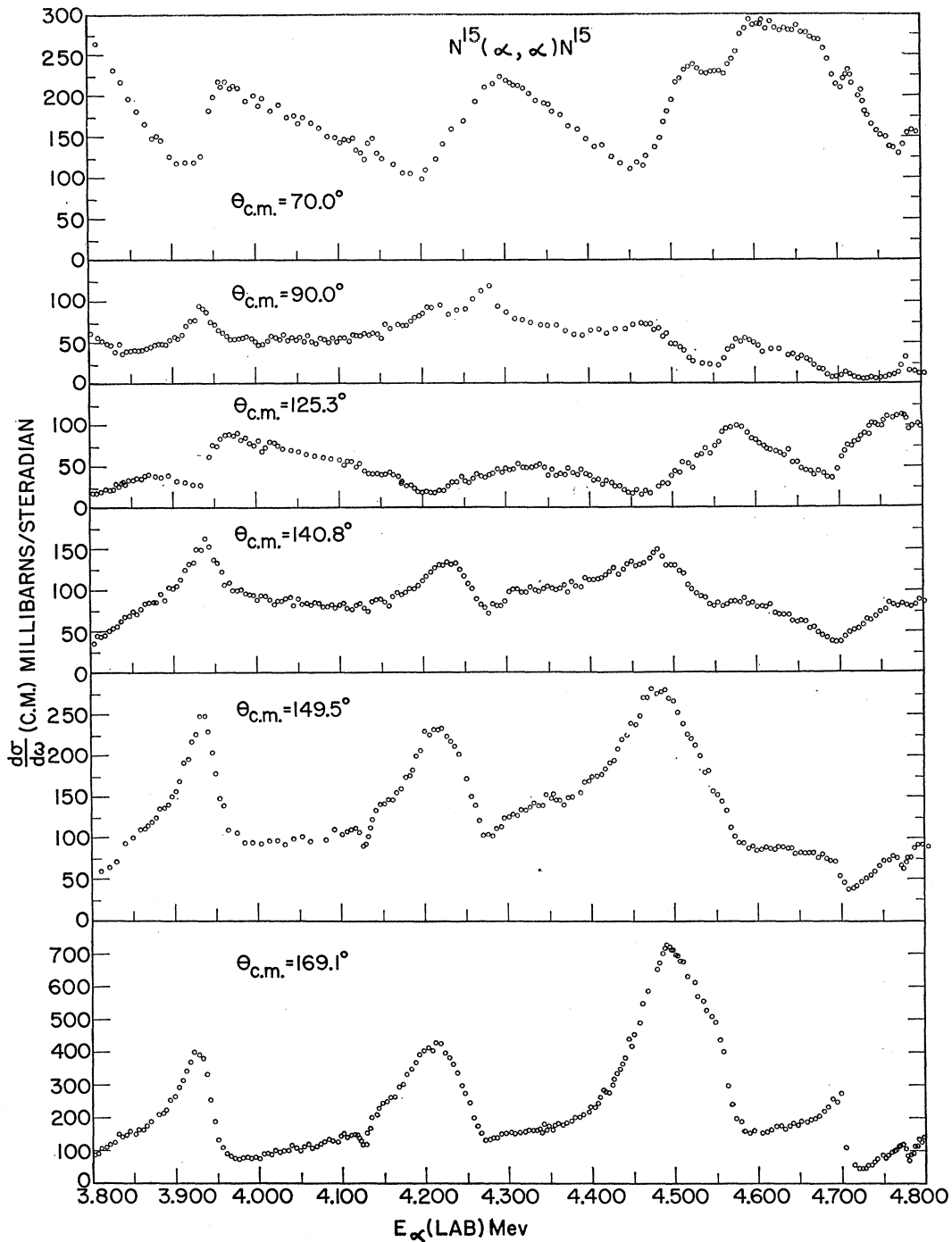
FIG. 5. Experimental cross sections from 3.8 Mev to 4.8 Mev.

which the N^{15} spin flips during the course of scattering. The latter scattering is incoherent with respect to Coulomb scattering.

The connection between the phase shifts and the parameters describing the compound nucleus is given by the R matrix of Wigner and Eisenbud.[22] For the case of one energetically possible channel and many levels of

the same J value and parity, the formula is

$$\delta_l^{\pm} = \tan^{-1}\left(\frac{k/A_l^2}{\Delta_{\lambda l}/\gamma_{\lambda l}^2 + [\sum_n \gamma_\lambda \ln^2/(E_{\lambda n}-E)]^{-1}}\right)$$

$$-\tan^{-1}\left(\frac{F_l}{G_l}\right)_{r=a_c}. \quad (4)$$

[22] E. P. Wigner and L. Eisenbud, Phys. Rev. **72**, 29 (1947).

For the case of a single level, (4) reduces to the usual form:

$$\delta_l{}^{\pm}=\tan^{-1}\left(\frac{k/A_l{}^2}{\Delta_{\lambda l}/\gamma_\lambda l^2+[\gamma_\lambda l^2/(E_\lambda-E)]^{-1}}\right)$$
$$-\tan^{-1}\left(\frac{F_l}{G_l}\right)_{r=a_c}. \quad (5)$$

Expressions (4) and (5) are commonly written in the form

$$\delta_l=\beta_l-\phi_l, \quad (6)$$

where β_l is the resonant phase shift and ϕ_l the "potential" or "hard-sphere" phase shift. E_λ is the eigen-energy of the compound nucleus, and $\gamma_\lambda l^2$ is the reduced width. The reduced width is related to the experimentally measured level width $\Gamma_{\lambda l}$ by the expression

$$\Gamma_{\lambda l}=2[k\gamma_\lambda l^2/A_l{}^2]_{r=a_c}. \quad (7)$$

The quantities $\gamma_\lambda l^2$ and E_λ, which characterize the resonant levels of the compound system, are dependent on the interaction radius and on a non-energy-dependent boundary condition. The level shift parameter $\Delta_{\lambda l}$ in Eqs. (4) and (5) is a measure of the amount that the resonant energy, defined as $E_R=E_\lambda+\Delta_{\lambda l}$, is shifted from the characteristic energy E_λ of the compound system. $\Delta_{\lambda l}$ is given by the expression

$$\Delta_{\lambda l}=-\left[\frac{k\gamma_\lambda l^2}{\rho}\left(\frac{\rho}{A_l}\frac{dA_l}{d\rho}+l\right)\right]_{\rho=ka_c}. \quad (8)$$

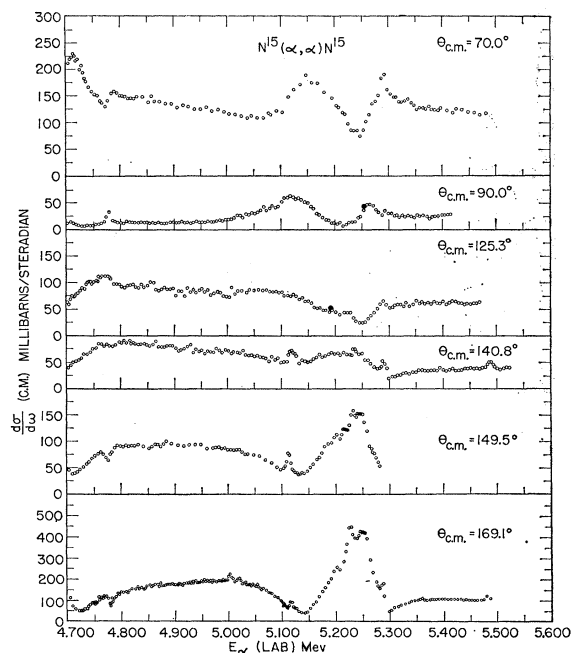The quantities F_l and G_l in the above expressions are the

FIG. 6. Experimental cross sections from 4.7 Mev to 5.5 Mev.

regular and irregular Coulomb wave functions[23] and the combination $A_l{}^2=F_l{}^2+G_l{}^2$ is the reciprocal of the Coulomb penetrability. The interaction radius is given to sufficient accuracy by the expression[24]

$$a_c=r_0(A_1{}^{\frac13}+A_2{}^{\frac13}). \quad (9)$$

In the present experiment r_0 was chosen equal to 1.40×10^{-13} cm, which leads to an interaction radius of 5.67×10^{-13} cm.

The general shape of the cross-section curve in the off-resonant region can be explained by the smoothly varying contributions from Rutherford scattering, potential scattering, and resonant scattering from nearby broad resonances.

While in most cases only the contributions from broad resonances have to be considered in fitting the experimental data in the off-resonant region, a situation can arise where the contribution of a seemingly far-off narrow resonance must also be considered. This unusual behavior of a narrow level occurs if the resonance falls in an energy region in which the Coulomb penetrability is a rapidly increasing function of energy. More specifically, since the numerator of Eq. (5) can increase at a sufficient rate to compensate for the increase in value of the denominator, the contribution to the resonant phase shift can remain relatively constant or even increase far from the resonance energy of the narrow level. To account for this type of behavior, contributions from all observed levels of the same J value and parity in the energy region analyzed were considered in obtaining the final phase shift used at a particular energy. To facilitate calculations, the approximate formula,

$$\delta_l{}^{\pm}=\tan^{-1}\left(\sum_n\frac{k\gamma_{\lambda n}{}^2/A_l{}^2}{E_{\lambda n}+\Delta_{\lambda l}-E}\right)-\tan^{-1}\left(\frac{F_l}{G_l}\right)_{r=a_c}, \quad (10)$$

was used. The sum is over all levels of the same J value. This formula which is applicable at energies whose distance from the resonant energies of the levels included is large compared to the widths of these levels is an approximation to the correct multilevel formula, Eq. (4).

The broad levels were not sufficiently isolated in general to make possible estimates of the resonant energies and widths from the cross-section data. It was therefore not practicable to generate directly a series of phase shifts using Eq. (5) which would lead to a fit of the experimental data. The procedure followed was to extract phase shifts from the data through a point by point application of the cross-section relation Eq. (1) and then require that this series of phase shifts be associated with a particular E_λ and $\gamma_\lambda l^2$. This latter procedure can be simplified by rewriting the expression for

[23] I. Bloch et al., Revs. Modern Phys. 23, 147 (1951); W. T. Sharp, H. E. Gove, and E. B. Paul, Chalk River Report AECL-269 (unpublished).
[24] A. M. Lane and R. G. Thomas, Revs. Modern Phys. 30, 257 (1958).

TABLE II. Summary of results for levels for which spin and parity assignments have been made.

E_R (lab) (Mev)	Excitation energy of F¹⁹ [a] (Mev)	J^π	Γ_λ (lab) (kev)	E_λ (Mev)	$\gamma_\lambda{}^2$ (Mev-cm×10¹³)	$\left(\dfrac{\gamma_\lambda{}^2}{3\hbar^2/2\mu a}\right)$ (%)
1.878	5.475	3/2⁺	4	5.143	0.713	20.4
2.614	6.056	5/2⁺	1.5	6.012	0.327	9.3
2.635	6.073	5/2⁻	5	6.037	0.210	6.0
2.833	6.229	1/2⁺	10	6.208	0.106	3.0
2.883	6.269	5/2⁺	3	6.233	0.332	9.5
2.944	6.317	7/2⁺	3	6.288	0.280	8.0
3.07	6.41	1/2⁻	358	6.14	1.27	36.3
3.194	6.514	1/2⁺	5	6.510	0.0282	0.81
3.229	6.541	5/2⁺	2	6.535	0.0929	2.7
3.525	6.776	3/2⁻	3	6.748	0.0219	0.63
3.587	6.825	5/2⁺(3/2⁺)	1.5	6.825	0.0181	0.52
3.648	6.872	5/2⁻	35	6.866	0.217	6.2
3.705	6.917	9/2⁻(7/2⁻)	3	6.908	0.292	8.4
3.78	6.97	1/2⁻	64	6.94	0.175	5.0
3.92	7.08	7/2⁺	~40	7.11	0.596	17.0
3.94	7.10	3/2⁺	~10	7.10	0.0253	0.72

[a] Excitation energies were computed from the mass values given by A. H. Wapstra, Physica **21**, 367 (1955).

the resonant phase shift [see Eq. (5)] in the form:

$$E = E_\lambda + F(E)\gamma_\lambda l^2, \qquad (11a)$$

where

$$F(E) = \frac{\Delta_{\lambda l}}{\gamma_\lambda l^2} - \frac{k/A l^2}{\tan\beta_l}. \qquad (11b)$$

Equation (11a) defines $F(E)$ as a linear function of energy, E. Equation (11b) relates $F(E)$ directly to the data through $\tan\beta_l$. The procedure for obtaining E_λ and $\gamma_\lambda l^2$ now reduces to a simple straight-line fit of a plot of $F(E)$ vs E. The slope of the line gives the value of $\gamma_\lambda l^2$, and E_λ is the energy for which $F(E)=0$. An illustration of this procedure, as applied to the S resonance at 3.07 Mev, is shown in Fig. 7.

In analyzing the narrow resonances, the following simplified expression was used for the phase shift:

$$\delta_l^\pm = \tan^{-1}\left(\frac{\Gamma/2}{E_\lambda - E}\right) - \tan^{-1}\left(\frac{F_l}{G_l}\right)_{r=a_c}. \qquad (12)$$

This single-level expression is applicable to narrow resonances where $A l^2$ and the level shift $\Delta_{\lambda l}$ are approximately constant over the width of the resonance. The procedure followed was to estimate the resonant energy and level width from the data and then to generate a series of phase shifts with the above expression. The detailed fitting of the cross-section curves was then carried out using the vector method described by Laubenstein and Laubenstein.[25,26]

B. Fit to Experimental Data

The region of excitation from approximately 1.75–3.51 Mev is characterized by a broad S resonance at 3.07 Mev and a series of narrow resonances. The broad

[25] R. A. Laubenstein and M. J. Laubenstein, Phys. Rev. **84**, 18 (1951).
[26] L. J. Koester, Phys. Rev. **85**, 643 (1952).

resonance was analyzed using the technique described in Sec. A. The resulting parameters are given in Table II. In analyzing all the narrow levels with the exception of the $P_\frac{1}{2} - F_\frac{5}{2}$ doublet at 3.194 and 3.229 Mev, it was possible to use the vector method with the contributions from all other resonances considered constant over the resonance being analyzed. In the case of the $P_\frac{1}{2} - F_\frac{5}{2}$ doublet, however, the resonance energies fall very near to the resonance energy of the broad S resonance at 3.07 Mev; it was necessary, therefore, to consider the S contribution as a variable over the width of the doublet.

The fit to the region from approximately 3.50 to 3.95 Mev is determined by the assignments made for the three broad levels at 3.648, 3.78, and 3.92 Mev. The analysis of this region is complicated since these three broad levels lie within an energy region of approximately 300 kev. This situation results in considerable distortion to the true shapes of the resonances.
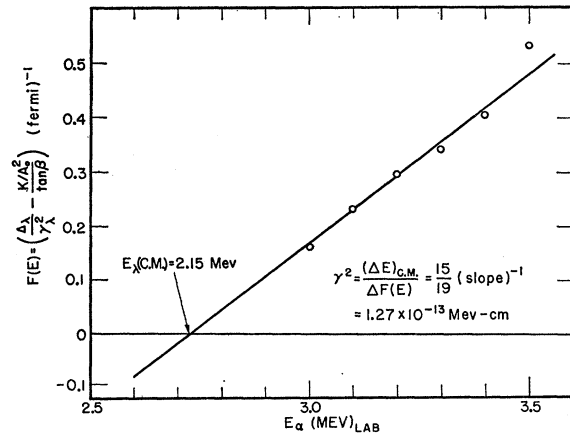
The spin assignment of the level at 3.648 Mev was

FIG. 7. Straight-line fit of $F(E)$ vs E curve for the 3.07-Mev resonance to illustrate the determination of $\gamma_\lambda{}^2$ and E_λ.

TABLE III. Summary of positions of levels observed for which no spin and parity assignments have been made.

E_R (lab) (Mev)	Excitation energy of F^{19*} [a] (Mev)	Γ_{lab} [b] (kev)
4.127	7.251	8
4.22	7.32	80
4.49	7.53	90
(4.53)[c]	(7.57)[c]	
4.700	7.703	30
4.780	7.766	8
4.93	7.88	260
(5.005)[c]	(7.944)[c]	(8)[c]
(5.018)[c]	(7.954)[c]	(5)[c]
5.116	8.031	8
5.203	8.100	8
5.232	8.123	6
5.25	8.13	65
5.284	8.164	10
5.481	8.320	10

[a] The mass values used to compute the excitation energy in F^{19} are taken from A. H. Wapstra, Physica 21, 367 (1955).
[b] The level widths are estimated from the data. They have not been corrected for beam energy spread and target thickness.
[c] Uncertain level.

made essentially on the basis of the 90-degree data. At all angles, with the exception of 90 degrees, it was possible to obtain a fit with either a $D_{\frac{3}{2}}$ or a $D_{\frac{5}{2}}$ assignment, but at 90 degrees only a $D_{\frac{5}{2}}$ assignment would give sufficient peak height to fit the data. The width and resonance energy of this level were determined primarily by the behavior at 125.3, 140.8, and 149.5 degrees. Since the 125.3-degree data are due to incoherent scattering [see Eq. (1c)], the resonance is represented by a nearly symmetric peak centered at the resonant energy. It is possible, therefore, to obtain a good estimate of the width and resonance energy for the resonance at this angle. The 140.8- and 149.5-degree data are important because the Legendre polynomial for $l=2$ is relatively large and therefore the fit at these angles is sensitive to the amount of D-wave phase shift. The reported values of width, 35 kev, and resonance energy, 3.648 Mev, are a compromise estimate based on a good fit for all angles.

The most definite evidence for the presence of an S resonance at 3.78 Mev is the rapid falloff of the resonance curve at 90 degrees for energies greater than 3.7 Mev. The possibility that this anomaly may be due to an $l=2$ resonance is eliminated on the basis of shape and magnitude of the cross section. The possibility that the effect is attributable to $l=4$ is eliminated by considering the Wigner limit on the reduced width for an $l=4$ resonance, $(\gamma_\lambda^2 \leq \frac{3}{2}\hbar^2/\mu a_c)$.[27] The width of an $l=4$ resonance would have to be of the order of 60 kev to fit the decrease in cross section. This width, however, would exceed the Wigner limit by more than 100%, and is thus unlikely. In fitting this resonance the effect of the S resonance at 3.07 Mev was considered.

The anomaly which appears as a single resonance at approximately 3.92 Mev is actually a closely spaced F

[27] T. Teichmann and E. P. Wigner, Phys. Rev. 87, 123 (1952).

and P doublet. It was possible to establish the spin of the P resonance as $\frac{3}{2}$ from the data at 140.8 degrees where the coherent scattering contribution for $l=3$ vanishes. The spin assignment of $F_{7/2}$ for the $l=3$ resonance was chosen since only the combination of $F_{7/2}$ and $P_{\frac{3}{2}}$ gives sufficient peak height at 169.1 degrees. Approximate values of 3.92 Mev and 40 kev for the resonance energy and width were picked for this level so as to produce a fit in the 3.6 to 3.8 Mev region at angles which are sensitive to the F contribution.

The $D_{\frac{3}{2}}$ level at 3.525 Mev was the only narrow level between 3.5 Mev and 3.8 Mev for which a definite spin assignment could be made. This level was sufficiently removed from the three broad levels mentioned above to be relatively unaffected by variations in the parameters assumed for the broad levels. In the case of the F resonance at 3.587 Mev and the G resonance at 3.705 Mev, while definite l-value J assignments could be made on the basis of shape, it was felt that definite assignments could not be given since the fits of these levels were very dependent on the rather complicated system of broad levels mentioned above. It is possible, however, to assign J values to these levels which will lead to a good fit of the narrow levels and still preserve the fit to the broad levels. An $F_{\frac{5}{2}}$ assignment gave the best fit in the off-resonance region at 169.1 degrees and also led to a better fit at 125.3 degrees. The only contribution of the G resonance to the cross section at 149.5 degrees is from incoherent scattering. An indication of the correct assignment is obtained by combining the two possible incoherent G contributions with the incoherent contribution of the neighboring $D_{\frac{5}{2}}$ resonance. If this is done, a significantly better fit is obtained with a $G_{9/2}$ assignment.

The resonances above 4.0-Mev bombarding energy have not as yet been assigned spins and parities. Approximate values for the resonant energies and widths of these levels have been estimated from the data and are shown in Table III.

V. RESULTS AND CONCLUSIONS

Thirty resonances corresponding to virtual levels in F^{19} have been observed in a study of the elastic scattering of alpha particles by N^{15} from 1.75- to 5.50-Mev bombarding energy. The energy levels found in $N^{15}(\alpha,\alpha)N^{15}$, as well as levels in the same energy range found through other experiments, are shown in Fig. 8.

A phase-shift analysis of the cross-section curve from 1.85 Mev to 4.00 Mev yielded the values for the resonant energies, spins and parities and reduced widths of the levels in this energy range. The results of the analysis are given in Table II. In cases where it was not possible to make a definite choice of spin, the less likely assignments have been indicated by enclosure in parentheses. Values for the excitation energy and the characteristic energy E_λ are given with respect to the F^{19} ground state.
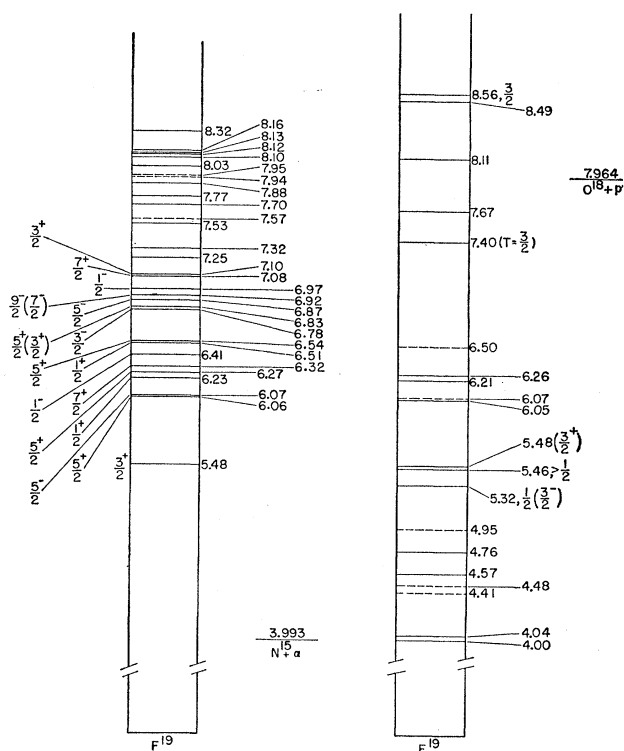
FIG. 8. Energy levels of F¹⁹. Levels found in the present experiment are shown in the energy level diagram on the left. The energy level diagram on the right shows the information available from other experiments.

An assignment of $\frac{3}{2}^+$ was strongly suggested for the 5.476-Mev level found by Price[9] through the experiment $N^{15}(\alpha,\gamma)F^{19}$. This assignment is fully confirmed by the present experiment. An additional level reported by Price at 5.455-Mev excitation, having a width less than 1 kev, was too narrow to be resolved. Harlow et al.,[10]

who studied the reaction $O^{18}(d,n)F^{19}$, using the "counter ratio method," reported a level at 6.18 Mev. This level was tentatively assigned a spin of either $\frac{3}{2}$ or $\frac{1}{2}$. It is probable that this level corresponds to our $\frac{1}{2}^+$ level at 6.23 Mev. The level at 6.07 Mev was observed by Hossain and Kamal[12] in the inelastic scattering of protons from F^{19}. These workers also made a doubtful identification of a level at 6.50 Mev. Both the level at 6.07 Mev and the level at 6.50 Mev, which is actually a closely spaced doublet, were observed in the present experiment. More recently, Butler et al.[11] have studied the excited states of F^{19} by observing γ-ray thresholds in the $O^{18}(d,n\gamma)F^{19}$ reaction. This work has lead to the identification of levels at 6.05, 6.21, 6.26, 7.40, 7.67, and 8.11 Mev. With the exception of the 7.40-Mev level, these levels are in close agreement with levels found in the present experiment. As is pointed out by Butler et al., the absence of the 7.40-Mev level may be explained if it has an isotopic spin of $\frac{3}{2}$.